

# A Wafer-Scale MEMS & Analog VLSI System for Active Drag Reduction

Bhusan Gupta, Rodney Goodman, Fukang Jiang, Tom Tsao, Yu-Chong Tai  
Dept. of Electrical Engineering  
California Institute of Technology  
Pasadena, CA 91125

Steve Tung, Chih-Ming Ho  
MANE  
UCLA  
Los Angeles CA 90024

E-mail: bgupta@caltech.edu

## Abstract

We describe an analog CMOS VLSI system that can process real-time signals from integrated shear stress sensors to detect regions of high shear stress along a surface in an airflow. The outputs of the CMOS circuit control the actuation of integrated micromachined flaps with the goal of reducing this high shear stress on the surface and thereby lowering the total drag. We have designed, fabricated, and tested components of this system in a wind tunnel in both laminar and turbulent flow regimes with the goal of building a wafer-scale system.

## 1: Introduction

In today's cost-conscious air transportation industry, fuel costs are a substantial economic concern. Drag reduction is an important way to increase fuel efficiency which reduces these costs. It is estimated that even a 5% reduction in drag can easily translate into savings of millions of dollars in annual fuel costs.

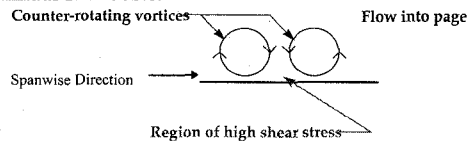


**Figure 1** Diagram showing the interaction of a vortex pair and the wall illustrating the high shear stress (hence drag) region created by the pair of counter-rotating streamwise vortices.

Organized structures which play an important role in turbulence transport may cause large skin friction drag. Commonly observed near-wall streamwise vortices cause high drag in turbulent flows (Figure 1). The interaction of these vortices, which appear randomly in both space and time, with the viscous layer near a surface creates regions of high surface shear stress. This shear stress, when integrated over a surface, contributes to the total drag. Attempts to reduce drag by controlling turbulent flows have focused on methods of either preventing the formation or mitigating the strength of these vortices. The microscopic size of

these vortices, which decreases as the Reynolds number of the flow increases, has limited physical experimentation, and the inherent complexity of the non-linear Navier-Stokes equations has likewise limited the analytical approaches.

## 2: How Small Is Small?

By examining shear stress patterns in our wind tunnel at velocities between 10 and 20 m/s, one can narrow the scope of the problem in order to extract useable statistics. The drag-inducing vortex pair streaks vary as the Reynolds number of the flow changes. For a typical airflow of 15 meters per second (54 km/hr) in the wind tunnel, the Reynolds number is about  $10^4$ . This, in turn, gives the vortex streaks a statistical mean width of about 1 millimeter. The length of a typical vortex streak can be about 2 centimeters giving the streaks a twenty to one aspect ratio. The average spacing between streaks is about 2.5 millimeters. The mean rate of appearance of the streaks is approximately 100 Hz. The appearance and disappearance of these vortex pairs can be best be described by a chaotic process.

## 3: Computer simulations

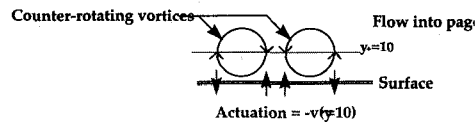


**Figure 2** Simple control law which demonstrates the required actuation at the wall boundary to achieve a significant drag reduction.

Numerical simulations demonstrate that suppressing the interaction between stream-wise vortices and the wall [1] achieves significant drag reduction (on the order of about 25%). These computational fluid dynamics' experiments incorporate active feedback control to achieve this goal.

The control scheme used in the experiments involved blowing and suction at the wall according to the normal component of the velocity field. This normal component is sensed in the near-wall region away from the surface (see Figure 2). It appears that a simple control law that pushes the areas of high shear stress away from the wall is beneficial to minimizing the overall drag. This observation forms the basis for the system that we wish to build.

## 4: System Details

We want to combine the technologies of silicon micromachining and analog VLSI to build an integrated wafer-scale system which actively strives to reduce the drag along its surface. Micromachining technology allows construction of fluid sensors and actuators on the same scale as the vortex pairs. Analog VLSI affords us the ability to build dense circuits which do the real-time processing necessary for an integrated system.

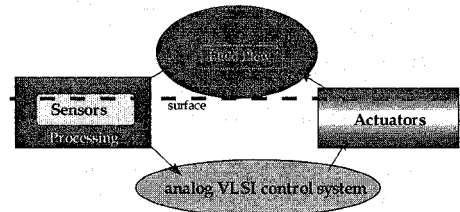


**Figure 3** Schematic diagram of our proposed system.

The goal is to design a system (Figure 3) that incorporates VLSI control circuitry along with microscopic sensors and actuators and control circuitry that can actively deform its surface to reduce drag.

Circuits process the signals from the sensors to find regions of high shear stress. This detection process uses information about the spatial and temporal nature of the streaks. First, the long and narrow aspect ratio leads to building "column"-oriented templates for streak detection. We organize the sensor outputs into thin feature detectors oriented in the direction of the airflow. When several sensors in a column register either a larger or smaller output than their neighbors in a spanwise direction, this difference accumulates. If this accumulated difference exceeds a threshold, a vortex pair streak may be present in that column. The appropriate control action raises the associated actuator.

## 5: Micromachined Components

Silicon micromachining technology is utilized to build the microsensors and microactuators [2,3,4]. The details of the sensors and actuators are covered elsewhere but are briefly included here for completeness.

### 5.1: Shear Stress Sensor:

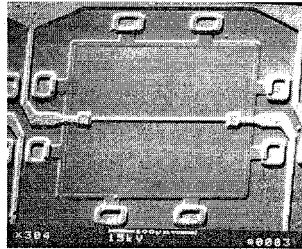


**Figure 4** Shear stress sensor showing the polysilicon transducer element over the silicon nitride diaphragm.

The microsensor (Figure 4) allows measurement of the heat transfer between a heated wire and the air. Heat transfers by convection from the electrically heated wire to the fluid flow causing a power change in the polysilicon wire. The sensors used in this experiment have been fabricated as a single row of 25 sensors. This allows continuous monitoring of a spanwise section of the wind tunnel. This sensor allows us, for the first time, to record the instantaneous shear stress associated with the near wall structures.



**Figure 5** Array of 25 shear stress sensors which span a distance of 7.5mm.

### 5.2: Microactuator:

The microactuator (Figure 6) [5] is a thin plate that is raised via both magnetic and thermal actuation. Current through the coil of metal on the flap interacts with an external magnetic field to cause up to a 100 $\mu$ m vertical deflection.

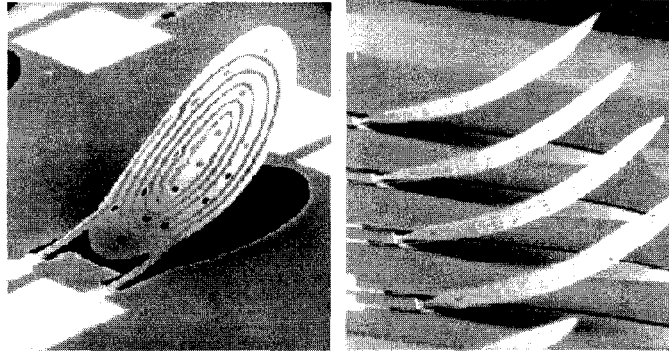


**Figure 6** Photograph of a microactuator and an array of microactuators. The actuator measures about 300 $\mu$ m by 500 $\mu$ m.

### 5.3 Wafer Integration

Our goal is to build a completely integrated system so the fabrication processing for both the shear stress sensor and microactuator is chosen to be compatible with the CMOS circuitry. We intersperse the micromachining steps with the CMOS process steps so that we do not impair either part. Because of the complexity involved in this system, we split the process flow among two different fabrication facilities. The 2.0 $\mu$ m double polysilicon CMOS processing is done in the Microlab at the University of California at Berkeley. The micromachining processing is carried out at the fabrication facility at Caltech.

The wafers start out at Berkeley with the first sixteen steps of the CMOS process up to metalization. The wafers then come to Caltech for the first round of micromachining steps primarily centered around the sensor. For instance, the nitride which is used as the sensor diaphragm material has to be deposited before the CMOS aluminum otherwise the high temperature would cause the aluminum to melt. The wafers then go back to Berkeley for metalization. The wafers then come back to Caltech for the actuator processing. This is the last set of processing steps because the actuator requires a release step which then makes any further processing difficult. The combined process flow requires about 32 masks and over 65 different processing steps. The overall process has four polysilicon and five metal layers.

## 6: Control Circuit

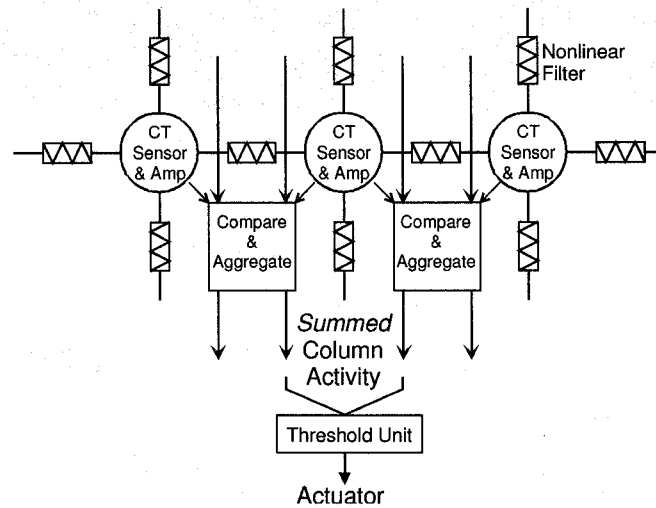


**Figure 7** Block diagram of the complete detection/control architecture.

Figure 7 shows a diagram of how the information is processed in the detection/control chip. A non-linear filtering network connects together the amplified outputs of the shear stress sensors. The filtering preserves large differences between adjacent sensors while smoothing small differences. The comparison and aggregation is organized by columns corresponding to different actuators. Once the signal is aggregated and exceeds a threshold then the actuator is driven. The general design methodology for the circuits is described in [6].

## 7: Prior Results

We have built previous versions of the system that use separate substrates for the sensor, control circuitry, and actuator. In this discrete system, we have been able to check the functionality and performance of our design. Figure 8 plots the response from the control circuitry versus the measured instantaneous shear stress. The plot demonstrates that the large shear stress values trigger the actuator. Figure 9 shows a plot of the full 25 sensor field and the reduced five-sensor field used to generate the detection/control output.

## 8: Wafer Scale System

We expect to have results of our wafer-scale system soon. The wafer consists of the same die replicated many times (Figure 10). The die contains both the sensors, actuators, and VLSI control circuitry.

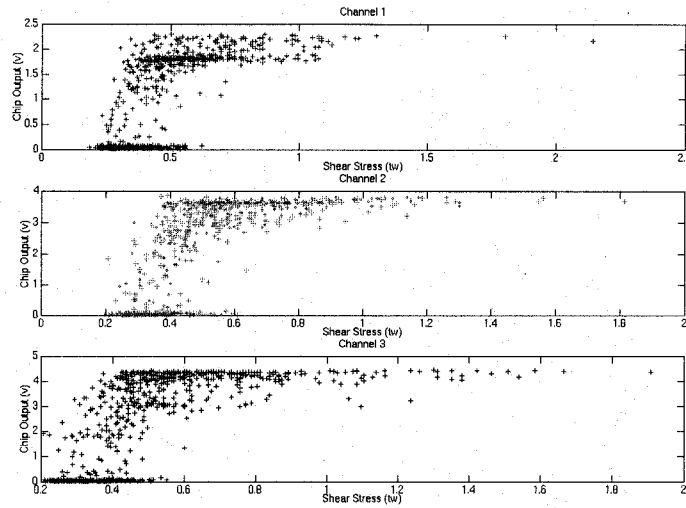


**Figure 8** Transfer curve for three channels of the prior detection/control chip with the data recorded at 15 m/s. The data indicates that for large values of shear stress, the detection and control circuitry would, in fact, turn on an actuator.

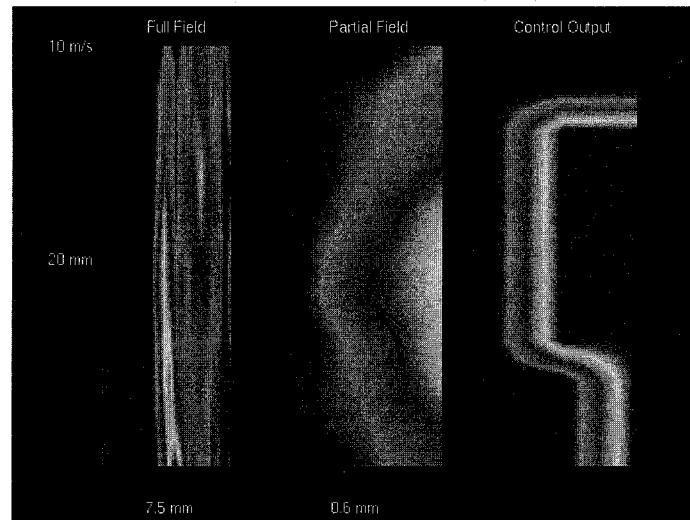


**Figure 9** Two dimensional flow picture of instantaneous shear stress. From left to right we plot the full span (25 sensor) recording, an enlargement of the middle three sensors, and finally, the output of the detection/control chip corresponding to those three inputs. We record the data in a turbulent flow regime with a free stream velocity of 10 m/s. We obtain the two dimensional aspect of the plots by time sampling a one dimensional span. The lighter greyscale values correspond to higher values.

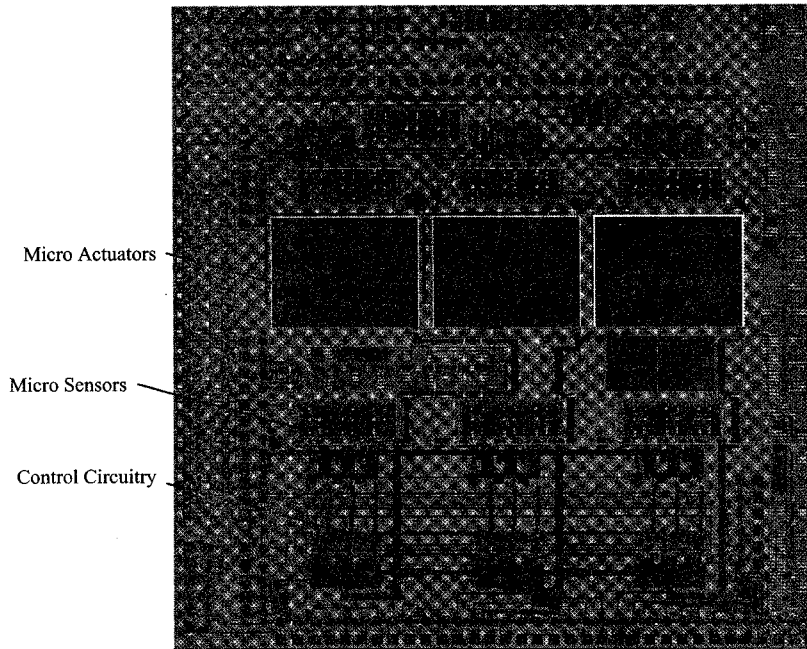


**Figure 10** Plot of one die of a wafer-scale implementation

**Acknowledgments:**

This work is supported in part by the Center for Neuromorphic Systems Engineering as a part of the National Science Foundation Engineering Research Center Program under grant EEC-9402726; and by the California Trade and Commerce Agency, Office of Strategic Technology under grant C94-0165. This work is also supported in part by ARPA/ONR under grant no. N00014-93-1-0990, and by an AFOSR University Research Initiative grant no. F49620-93-1-0332.

**References**

- [1] P. Moin, J. Kim, H. Choi, "On Active Control of Wall-Bounded Turbulent Flows," AIAA Paper No. 89-0960, 1989.
- [2] P.R. Bandyopadhyah, "Development of a Microfabricated Surface for Turbulence Diagnostics and Control," *ASME Application of Microfabrication to Fluid Mechanics*, Chicago (1994), pp. 67-74.
- [3] C. Liu, Y.C. Tai, J.B. Huang, C.M. Ho, "Surface Micromachined Thermal Shear Stress Sensor," *ASME Application of Microfabrication to Fluid Mechanics*, Chicago (1994), pp. 9-15.
- [4] F. Jiang, Y.C. Tai, J.B. Huang, C.M. Ho, "Polysilicon Structures for Shear Stress Sensors," to be published in *Tech. Digest IEEE TENCON '95*, Hong Kong, Nov. 1995.
- [5] T. Tsao, C. Liu, Y.C. Tai, C.M. Ho, "Micromachined Magnetic Actuator for Active Fluid Control," *ASME Application of Microfabrication to Fluid Mechanics*, Chicago (1994), pp. 31-38.
- [6] C.A. Mead, *Analog VLSI and Neural Systems*, Addison-Wesley, Reading, Massachusetts (1989).